

Temporal evolution of neural activity and connectivity during microsleeps when rested and following sleep restriction

Govinda R. Poudel^{a,b,c,*}, Carrie R.H. Innes^{a,b}, Richard D. Jones^{a,b,d,e,f}

^a New Zealand Brain Research Institute, Christchurch, New Zealand

^b Department of Medical Physics and Bioengineering, Christchurch Hospital, Christchurch, New Zealand

^c Sydney Imaging, Brain and Mind Centre, The University of Sydney, NSW, Australia

^d Department of Electrical and Computer Engineering, University of Canterbury, Christchurch, New Zealand

^e Department of Psychology, University of Canterbury, Christchurch, New Zealand

^f Department of Medicine, University of Otago, Christchurch, New Zealand

ARTICLE INFO

Keywords:

Sleep deprivation

Dynamic functional connectivity

fMRI

Microsleeps

ABSTRACT

Even when it is critical to stay awake, such as when driving, sleep deprivation weakens one's ability to do so by substantially increasing the propensity for microsleeps. Microsleeps are complete lapses of consciousness but, paradoxically, are associated with transient increases in cortical activity. But do microsleeps provide a benefit in terms of attenuating the need for sleep? And is the neural response to microsleeps altered by the degree of homeostatic drive to sleep? In this study, we continuously monitored eye-video, visuomotor responsiveness, and brain activity via fMRI in 20 healthy subjects during a 20-min visuomotor tracking task following a normally-rested night and a sleep-restricted (4-h) night. As expected, sleep restriction led to an increased number of microsleeps and an increased variability in tracking error. Microsleeps exhibited transient increases in regional activity in the fronto-parietal and parahippocampal area. Network analyses revealed divergent transient changes in the right fronto-parietal, dorsal-attention, default-mode, and thalamo-cortical functional networks. In all subjects, tracking error immediately following microsleeps was improved compared to before the microsleeps. Importantly, post-microsleep recovery in tracking response speed was associated with hyperactivation in the thalamo-cortical network. The temporal evolution of functional connectivity within the frontal and posterior nodes of the default-mode network and between the right fronto-parietal and default-mode networks was associated with temporal changes in visuomotor responsiveness. These findings demonstrate distinct brain-network-level changes in brain activity during microsleeps and suggest that neural activity in the thalamo-cortical network may facilitate the transient recovery from microsleeps. The temporal pattern of evolution in brain activity and performance is indicative of dynamic changes in vigilance during the struggle to stay awake following sleep loss.

Introduction

Microsleeps intrude into wakefulness when the drive to sleep is increased due to sleep deprivation (Chee and Tan, 2010; Doran et al., 2001; Goel et al., 2009; Innes et al., 2013; Ong et al., 2015) or due to extended-task monotony combined with a circadian dip (e.g., during post-lunch hours) (Peiris et al., 2006; Poudel et al., 2014). Microsleeps are hazardous in occupational settings, such as driving, as they are accompanied by complete lapses of responsiveness for 0.5–15 s and transient full or partial eye-closure (Ong et al., 2015; Peiris et al., 2006; Poudel et al., 2014). Although microsleeps are distinct transient events, they are concomitant with tonic performance variability, attention

lapses, and errors of commission, reflecting the underlying “wake-state instability” due to increased sleep drive (Doran et al., 2001). Whether intrusion of microsleeps during the struggle to stay awake provides any behavioural benefit remains unclear.

Evaluation of brain activity and performance surrounding clearly-defined microsleeps provides a framework to investigate the neuro-behavioural consequences of microsleeps, as done via EEG (Boyle et al., 2008; Davidson et al., 2007; Jonmohamadi et al., 2016; Toppi et al., 2016) and via fMRI (Ong et al., 2015; Poudel et al., 2014). We have previously demonstrated that microsleeps during extended continuous tracking tasks exhibit transient increases in activity in the fronto-parietal cortex and decreased activity in the bilateral thalamus (Poudel et al.,

* Corresponding author. Sydney Imaging, Charles Perkins Centre D17, Brain and Mind Centre, The University of Sydney, NSW, 2006, Australia.

E-mail address: govinda.poudel@sydney.edu.au (G.R. Poudel).

<https://doi.org/10.1016/j.neuroimage.2018.03.031>

Received 27 November 2017; Received in revised form 28 February 2018; Accepted 15 March 2018

Available online 16 March 2018

1053-8119/© 2018 Published by Elsevier Inc.

2014). Spontaneous eye-closures (behavioural manifestations of microsleeps) in sleep-deprived individuals also exhibit similar patterns of co-activation in frontal, parietal, and occipital brain areas (Ong et al., 2015). This large-scale co-activation in cortical systems during microsleeps has been attributed to cognitive resistance to falling asleep and neural modulations required for waking individuals from microsleeps (Poudel et al., 2014) or due to hypnagogic mentation during transition to sleep (Ong et al., 2015). Importantly, microsleep-related cortical co-activation patterns are distinct from those observed during voluntary eye-closures (Jonmohamadi et al., 2016; Ong et al., 2015; Poudel et al., 2010), suggesting attentional and arousal mechanisms at play during behavioural manifestations of microsleeps.

Further support for the involvement of cortical systems during increased sleep drive has been gained from research on attention lapses (prolonged response time) when sleep deprived. In particular, thalamic and visual processing capacity declines during drowsiness leading to attentional lapses on a selective attention task (Chee et al., 2008; Chee and Tan, 2010). A compromise in cortical capacity to down-regulate medial frontal and posterior cingulate activity led to prolonged reaction times in a vigilance task (Drummond et al., 2005). The cortico-thalamic alertness network can also show a compensatory response to sleep loss during complex tasks (Drummond et al., 2001; Tomasi et al., 2008) and even during the awake resting state (Poudel et al., 2012). The fronto-parietal and thalamic neural changes when attention and alertness are compromised following sleep loss (Chee et al., 2008; Chee and Tan, 2010; Tomasi et al., 2008) indicate that higher order cortical systems play an important role in regulating wakeful behaviour when arousal is compromised. However, the role of cortical networks in modulating wake-sleep behaviour in the face of increased sleep drive is not well understood. In particular, given the dangers associated with microsleeps in occupational settings, it is important to isolate the behavioural and neuronal processes during and after recovery from microsleeps.

In the current study, we recorded fMRI scans in 20 healthy participants performing a continuous visuomotor tracking task following both rested and sleep-restricted nights. We hypothesized that (i) microsleeps are associated with transient improvement in visuomotor performance, (ii) microsleeps after sleep restriction exhibit distinct neural response in cortical networks compared to microsleeps when rested, and (iii) transient changes in functional connectivity within the right fronto-parietal (rFPN), default-mode (DMN), and thalamo-cortical (TCN) networks are associated with loss of performance during microsleeps.

Materials and methods

Participants

Twenty right-handed volunteers (10 males and 10 females, aged 20–37 yr, mean age 24.9 yr) with no history of neurological, psychiatric, or sleep disorder participated in the study. For inclusion in the study, participants had to report a usual time to bed between 10 and 12 p.m. and a usual time in bed of 7.0–8.5 h. Ethical approval for the study was obtained from the New Zealand Upper South B Regional Ethics Committee (Ethics Reference Number: URB/09/02/005).

Study procedure

All participants visited the laboratory three times. On the first visit, they were briefed on the experimental protocol and provided with an Actiwatch (Respironics Inc., PA, USA) and a detailed sleep diary to record their sleep habits for 6 days and 5 nights prior to each of the two experimental sessions. They also recorded time of intake of caffeine, alcohol, and food in the diary. The second and third visits involved rested and sleep-restricted sessions, the order of which was counterbalanced across the participants. The sessions were 1 week apart to minimize residual effects of sleep restriction in participants who were sleep-restricted

during the first session.

Participants were asked to sleep normal hours during the week prior to the rested session. They were asked to do likewise for the sleep-restricted session except for the immediately preceding night in which their time-in-bed was restricted to 4 h (3:00–7:00 a.m.). Participants were requested not to engage in any safety-sensitive tasks (such as driving) following the sleep restriction. They were also asked not to consume any stimulants or depressants, such as alcohol, caffeine, and nicotine, on the day of either experimental session.

On the day of each scan, participants arrived at the laboratory an hour before the scanning session. Sleep habits recorded by the actiwatch and in the sleep diary were inspected prior to each of the scanning sessions to confirm compliance with the sleep schedule required for inclusion in the study. The sleep diary was used to confirm that participants did not consume any prohibited substances (caffeine and alcohol) on the day of scanning. Participants were provided with a lunch of hot noodles. They were also asked to rate their current subjective sleepiness using the Karolinska Sleepiness Scale (KSS) (Akerstedt and Gillberg, 1990) and Stanford Sleepiness Scale (SSS) (Hoddes et al., 1972) before entering the scanner room. Their self-rated propensity trait to fall asleep during the day was estimated using the Epworth Sleepiness Scale (ESS) (Johns, 1991). The participants entered the scanner between 1:00 p.m. and 2:30 p.m.

Experimental task

Each participant undertook a 20-min continuous pursuit-tracking task, which had been validated in our previous study (Poudel et al., 2014). During task performance, they had to manoeuvre an MR-compatible finger-based joystick (Current Designs, Philadelphia, PA, USA) to pursue a 2-D random target moving continuously on a computer screen (as described in Poudel et al. (2014)). Participants were familiarized with the tracking task for 2 min both inside and outside the scanner. They were instructed to control the joystick position so that the response disc was as close as possible to the centre of the moving target at all times. Foam support was placed below the right elbow for subject comfort and to minimize hand movement during tracking. Eye-video was used to monitor participant wakefulness during the tracking task.

Imaging procedure

All subjects were imaged using a Signa HDx 3.0 T MRI Scanner (GE Medical Systems) with an eight-channel head coil. High-resolution anatomical images of the whole brain were acquired using T1-weighted anatomical scans (repetition time: 6.5 ms; echo time: 2.8 ms; inversion time: 400 ms; field of view: 250 × 250 mm; matrix: 256 × 256; slice thickness: 1 mm). Functional images were acquired using echo-planar-imaging (repetition time: 2.5 s; echo time: 35 ms; field of view: 220 × 220 mm; slice thickness: 4.5 mm; number of slices: 37, matrix: 64 × 64, number of repetitions: 485 TR). The first five images of each session were discarded to allow for T1 equilibration. A magnetic field-map was acquired for each subject to reduce the functional image distortions (echo time: 4.0 ms and 6.2 ms). Participants were provided with ear plugs to lessen the high-volume acoustic noise from the scanner.

Preprocessing of MRI data

The MRI data were preprocessed using FSL (FMRIB's Software Library, www.fmrib.ox.ac.uk/fsl) and custom Linux Shell and Matlab scripts (Matlab 7.6.0, R2008a, Mathworks, MA, USA). fMRI preprocessing included motion correction (Jenkinson et al., 2002), field map-based unwarping (Jenkinson, 2003), slice-time correction, spatial smoothing with a 7-mm Gaussian kernel (full width at half maximum), and high-pass filtering with a cut-off of 128 s. The structural images were registered to the MNI152 standard space using a non-linear registration tool (FNIRT). Registration parameters produced by the non-linear

registration process were then used to warp the fMRI images into a standard $2 \times 2 \times 2 \text{ mm}^3$ Montreal Neurological Institute (MNI) template.

Data analysis

Detection of microsleeps

Microsleeps were defined behaviourally as in our previous work (Innes et al., 2013; Poudel et al., 2014). Briefly, a custom-built SyncPlayer™ program was used to replay synchronized eye-video, VEOG, and tracking target (x and y), response (x and y), speed, and tracking error. Any episodes of flat tracking (zero response speed) or divergences of response and target of 0.5–1.5 s duration accompanied by behavioural signs of drowsiness and full or partial (>80%) slow-eye-closures were marked as behavioural microsleeps. The response position, speed, and error signals were used to mark the onset and end of flat tracking responses. Eye-video were used as cues to mark the onset and end of eye-closure.

Analysis of visuomotor tracking performance surrounding microsleeps

Visuomotor tracking data was analysed in Matlab (Mathworks, USA) using custom scripts. The mean and standard deviation in tracking error (over the entire tracking period) before and after the removal of microsleeps were estimated. A moving average (60-s window and 1-s steps) was used to estimate second-to-second changes in tracking error during the rested and sleep-restricted sessions. The mean and standard deviation across participants in the moving average error were also estimated. Paired *t*-tests were used to compare means and standard deviations in tracking error when rested and sleep-restricted.

Tracking performance during 1.0-s epochs immediately before and after microsleeps was compared, with the start and end of microsleeps identified by manual rating. Alert episodes were defined as random 1.0-s episodes chosen from tracking period devoid of any microsleeps or tonic increase in tracking errors (identified by visually inspecting the tracking data). In each participant, the number of ‘alert episodes’ was chosen to be balanced by the same as the number of microsleeps. Average pre-versus post-microsleep tracking performances were compared using a paired *t*-test. To investigate the associations between tracking performance and microsleep duration we used Pearson's correlation where data was normally distributed and Spearman's correlation where data was not normally distributed. One-sample Kolmogorov-Smirnov test was used to test for the normality in the data.

Model-driven fMRI analysis

Participants were excluded from fMRI analyses if they had motion more than 3.0 mm of maximal translation or 1.0° of maximal rotation throughout the course of scanning. For each subject and session, general linear model (GLM) based analysis was used to identify the pattern of BOLD activity during microsleeps. The GLM comprised (i) duration modulated impulse regressors modelling BOLD activity during microsleeps, (ii) a normalized task-related error regressor modelling scan-to-scan BOLD fluctuations during scan-to-scan changes in tracking error (excluding periods just prior to and during microsleeps), and (iii) six motion parameters. Three participants in the sleep-restricted condition and one participant in the well-rested condition also had sleep episodes (longer than 15 s), which were modelled as separate regressors. The normalized tracking error regressor modelled average error during tracking for each TR (2.5 s) divided by average target speed during that time. All regressors were convolved with double-gamma haemodynamic response functions to model appropriate BOLD signal change. Appropriate contrasts were used to identify BOLD activity during microsleeps. Model driven analysis was implemented using FSL FEAT and run on MASSIVE infrastructure.

At the group level, the main effects of microsleeps (*t*-test) and of sleep restriction (paired *t*-test) on microsleep-related activity were estimated

using two separate models. A paired *t*-test was only conducted on the set of individuals who had microsleeps during both rested and sleep-restricted sessions. The models were estimated using non-parametric statistics (Randomize) using 5000 permutations. The main-effects of microsleeps on fMRI activity was considered significant at $p < 0.01$ (family-wise-error corrected using threshold free cluster enhancement (TFCE) technique). The stringent threshold ($p < 0.01$) was chosen to localise the BOLD fMRI activity with a higher spatial precision. The TFCE method enhances cluster-like features in statistical images (Smith and Nichols, 2009). Microsleep-specific activities were identified by masking out spatial regions involved in voluntary eye-closures (Poudel et al., 2010). A lenient threshold was used to identify differences in activity between microsleeps when rested and sleep restricted. Whole-brain analysis was conducted with statistical maps thresholded using clusters determined by $Z > 2.3$ and a (corrected) cluster significance threshold of $p < 0.05$.

We also performed regions of interest (ROI) analysis on regions selected from the parietal, frontal, and parahippocampal cortices to investigate whether sleep restriction changes the transient activity during sleep loss. These regions of interest have been shown to be modulated by sleep deprivation and microsleep duration in previous studies (Ong et al., 2015; Poudel et al., 2014). ROIs were defined using the group-level statistical maps of main-effects of microsleeps (via a group-level *t*-test) unbiased to rested or sleep restricted sessions. Spherical masks (10-mm diameter) centred on local maxima of activation during microsleeps (main effects of microsleep) were created for region-of-interest analyses. Parameter estimates obtained in first-level modelling of the effects of microsleeps were extracted from both rested and sleep-restricted sessions. Microsleep-related activity during rested and sleep-restricted sessions were compared using non-parametric Wilcoxon rank sum test and considered significant at $p < 0.05$.

Data-driven fMRI analysis

To investigate the dynamics of intrinsic networks during microsleeps following sleep restriction, we performed data-driven analysis using independent component analysis (ICA). MELODIC ICA (FSL) (Beckmann and Smith, 2004) was used to identify spatially-independent networks in each subject's fMRI data acquired during rested and sleep-restricted sessions. Total number of components in each subject were estimated using the Laplace approximation to the Bayesian evidence of the model order (Beckmann and Smith, 2004). Four distinct networks were identified in each subject: (i) default-mode network, comprising the ventromedial prefrontal cortex (vmPFC) and posterior-cingulate cortex (PCC), (ii) thalamic network, comprising the bilateral thalamus and visual cortices, (iii) dorsal-attention network, comprising the primary and secondary visual areas and parietal cortices, and (iv) right fronto-parietal network, comprising right inferior-frontal and posterior-parietal areas. The following steps were applied to identify these networks in each individual: (1) Standard-space spatial patterns underlying the 4 networks were obtained from previously published work (Smith et al., 2009), (2) MNI-space spatial maps were correlated with MNI-space transformed ICA maps from each individual subjects, (3) the within-subject ICA map, which was maximally spatially correlated (i.e., maximum *r* value) with the standard network, was used as subject-level map. This approach ensured spatial specificity of the maps used for each subject. Eigen-time-courses for each network were used to identify transient changes in the networks during microsleeps. The BOLD signal change (baseline corrected with the average signal from the two preceding points) time-locked to the microsleeps was deconvolved for each network of interest.

To investigate whether transient activity in each intrinsic network is associated with speed of recovery from microsleeps, we modelled post-microsleep activity during each microsleep using separate regressors (located at the end of microsleeps) convolved with the haemodynamic

response function. This generated a beta series reflecting strength of BOLD activity immediately at the end of microsleeps. To ensure that activity at the onset of microsleeps was separated from that at the end of microsleeps, we only used microsleeps of >5 -s duration for this analysis. The beta series were then correlated with change in response speed (post microsleep speed minus during microsleep speed) immediately following the end of microsleeps (1 s).

To investigate dynamics of changes in connectivity within and between the networks of interest, we used moving-window correlations to identify changes in functional connectivity within and between the networks. The four networks of interest were identified in each individual using MELODIC ICA, as described above, and average time-courses were extracted. Any effect of noise and microsleeps on the average time courses were regressed out using (i) 6 motion regressors, (ii) 3 regressors representing microsleeps and (iii) 3 regressors from ventricular CSF (using masks generated from segmentation using FSL). Any large transient deviations in time-series signal were also removed by removing any volumes with amplitudes >2.5 SD from mean. The removed volumes were replaced by interpolating data from nearby volumes. The pre-processed time-courses were band-pass filtered to 0.008–0.010 Hz to focus on low frequency fluctuations within the networks. For inter-network connectivity, the correlations between average time courses from each network of interest were estimated via moving-window correlations (step: 1 vol [2.5 s], window: 96 vol [4 min]), revealing temporal evolution of changes in functional connectivity. In each subject, this temporal dynamic was correlated with temporal changes in tracking performance estimated using moving-window averaging (step [2.5 s], window [4 min]). Furthermore, to estimate intra-network connectivity within right fronto-parietal and default-mode networks, individual-subject ICA maps were normalized to standard space and averaged. The maps were then manually thresholded to isolate the vmPFC, PCC, and right-frontal and right-parietal nodes within the networks. The moving-window-correlation approach was used to estimate intra-network connectivity, which was correlated with moving-window average changes in tracking performance.

Results

Microsleeps when rested and sleep-restricted

Three subjects were excluded from analysis due to excessive movement during fMRI scanning. Based on actigraphy analysis, we determined that the remaining participants ($N = 17$) had 7.84 ± 0.93 (mean \pm SD) hours of sleep during the night before the rested scan and 3.55 ± 0.21 h of sleep before the sleep-restricted scan (actual sleep hours). There was an increase in the mean number of microsleeps in the 20-min session following sleep-restriction (mean 27.9 vs 11.4, $t[15] = -2.10$, $p = .03$, 1-tailed). Of the 17 subjects, 15 had at least one microsleep during the sleep-restricted session, whereas only 7 had microsleeps when rested. There were increases in both the mean and SD of tracking errors following sleep restriction both before and after removing the effects of microsleeps (Fig. 1A) (all $p < 0.05$). As expected, tracking performance following sleep restriction was also highly variable (Fig. 1B).

Visuomotor performance in the moments surrounding microsleeps

Data from the sleep-restricted sessions were used to investigate the temporal dynamics of visuomotor performance surrounding microsleeps. There was a decrease in tracking error ($t = 3.6$, $p = 0.003$, paired t -test) immediately after the microsleeps (post-microsleep) relative to tracking error before microsleeps (pre-microsleep) (Fig. 2A). This decrease in tracking error was correlated (Pearson's $r = 0.42$, $p < 0.0001$) with duration of microsleeps (Fig. 2B). Of the 11 participants with ten or more microsleeps, 8 participants showed significant correlation between change in the tracking error and microsleeps duration ($p < 0.05$). The r -values ranged from -0.23 to 0.61, with standard deviation of 0.23. Whereas, only 4 showed significant correlation ($p < 0.05$) between pre-microsleeps tracking error and microsleeps duration. The r -values ranged from -0.07 to 0.71 with the standard deviation of 0.28.

Alert tracking, defined as random 1.0-s episodes chosen from tracking period devoid of any microsleeps or tonic increase in tracking errors, was

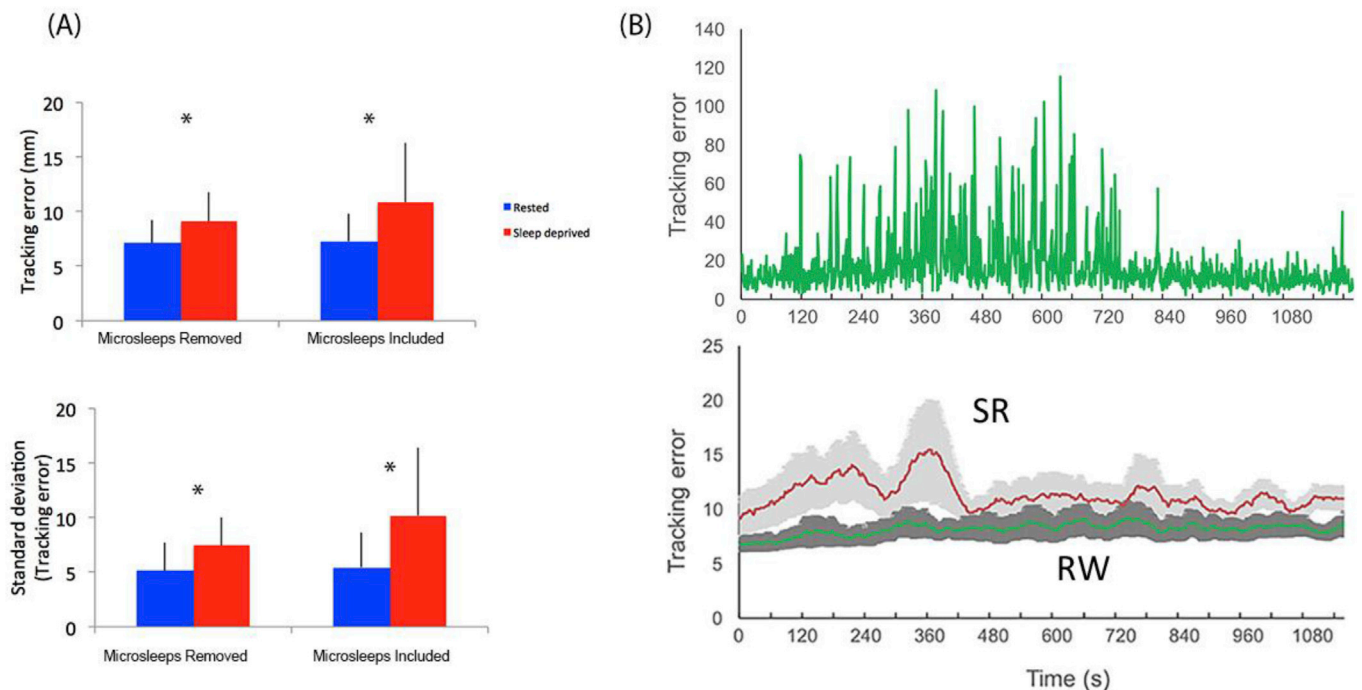


Fig. 1. Tracking performance in rested and sleep-restricted state. (A) Mean and standard deviation of tracking performance was increased in sleep-restricted compared to rested states both before and after the removal of microsleeps. (B) An example tracking performance in an individual with frequent microsleeps (top-panel) and average (and standard error) moment-to-moment changes in tracking performance (including standard error) in rested (RW, green) and sleep restricted (SR, red) sessions ($N = 17$). $*p < 0.05$.

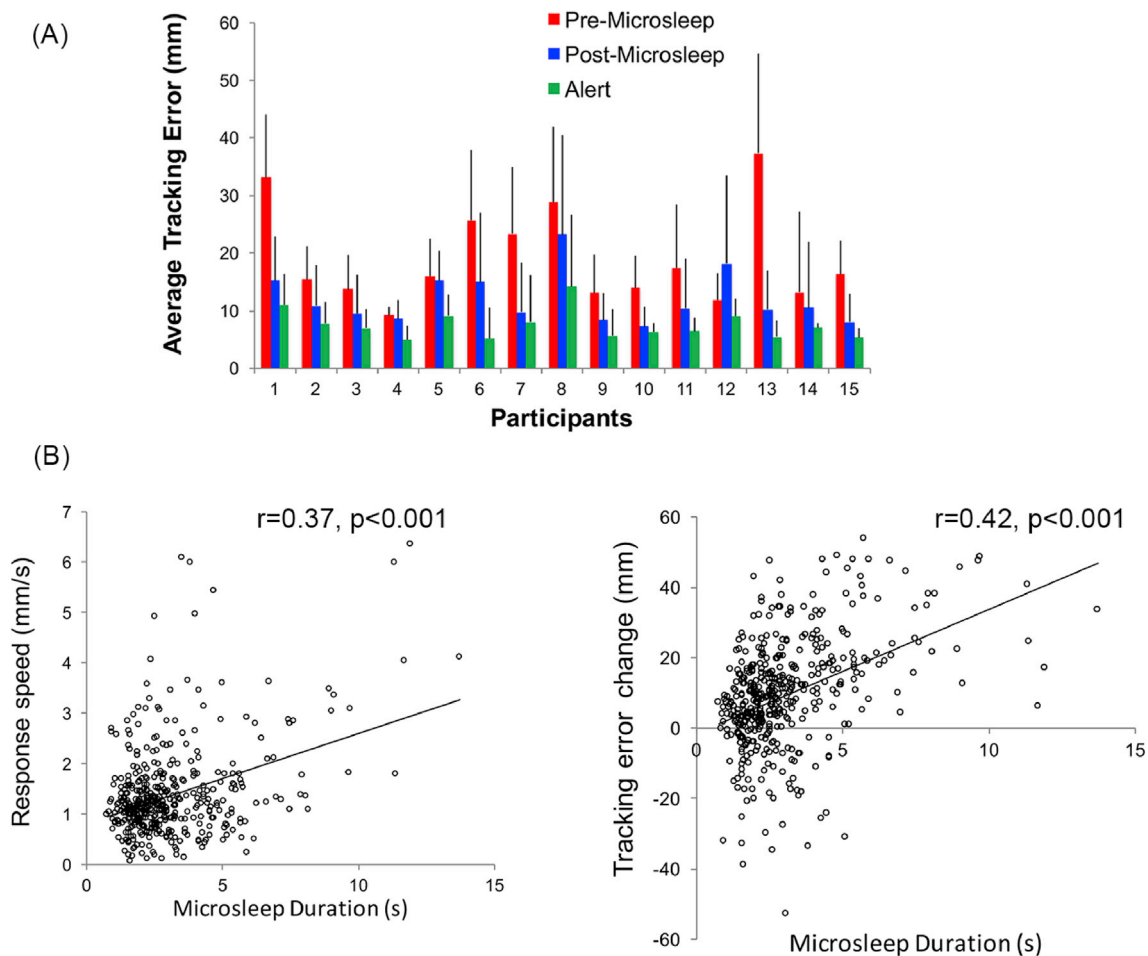


Fig. 2. (A) Average tracking performance pre- and post-microsleeps, and during alert tracking episodes in 15 subjects who had microsleeps during the sleep-restricted session. Alert tracking episodes were defined as random 1.0-s episodes chosen from tracking period devoid of any microsleeps or tonic increase in tracking errors. Error bars represent the standard deviation. (B) Scatter plots showing the correlation between microsleep duration and response speed and change in tracking error (pre-microsleep-post-microsleep) immediately following microsleeps.

better compared to both pre-microsleep ($t = 6.2$, $p < 0.001$) and post-microsleep ($t = 5.7$, $p < 0.001$) tracking performance. There was also a correlation (Pearson's $r = 0.37$, $p < 0.001$) between microsleep duration and response speed (Fig. 2B).

Regional brain activity during microsleeps

Group-level analysis revealed that microsleeps are associated with widespread increased activity in multiple cortical areas ($p < 0.01$, TFCE corrected), including the left inferior-frontal, bilateral superior-parietal, bilateral precentral, right posterior-parietal, and occipital cortices (Fig. 3, Table 1). Other brain regions with increased activity during microsleeps include the bilateral hippocampus and basal forebrain (subcallosal cortex).

Exploratory comparison of fMRI activity during microsleeps when rested and sleep-restricted

Only 5 subjects could be used in the analysis of fMRI activity of microsleeps when rested versus sleep-restricted as they had 5 or more microsleeps in both rested and sleep-restricted sessions. An exploratory whole-brain within-group comparison showed no difference between the increases in BOLD activity seen during microsleeps when sleep-restricted compared to rested. Post-hoc analysis on specific regions of interest revealed trends towards larger increases in the right superior-parietal and superior-frontal cortices when sleep-restricted. A larger increase

when sleep-restricted was significant only in the right superior-parietal lobe ($p = 0.02$) (Fig. 4). These findings should be interpreted with caution due to the small number of participants used.

Transient activity in large-scale networks during microsleeps

We identified intrinsic brain networks of interest during both rested and sleep-restricted sessions. Spatial correlations between subject-specific networks and spatial templates of resting-state networks were moderate to high (Pearson's $r > 0.4$). Time-resolved analysis of microsleep-related fMRI activity in these networks exhibited distinct temporal patterns of activity (Fig. 5). Visual inspection shows that the right fronto-parietal network (rFP) exhibited a transient increase when sleep-deprived compared to sustained activity when rested. In the default-mode network (DMN), microsleeps when sleep-deprived were associated with sustained reduced activity compared to increased activity when rested. In the dorsal-attention (DA) network, transient activity was observed in both rested and sleep-restricted microsleeps. Transient reduced activity was observed in the thalamic-visual network (TVN) when subjects were both rested and sleep-restricted.

For the thalamo-cortical networks, the beta series obtained from modelling the post-microsleep activity was correlated (Spearman's $r = 0.43$, $p = 0.003$) with the change in response speed at the end of microsleeps (response speed post microsleep-response speed during microsleep). There was no correlation between beta series from other networks and change in response speed.

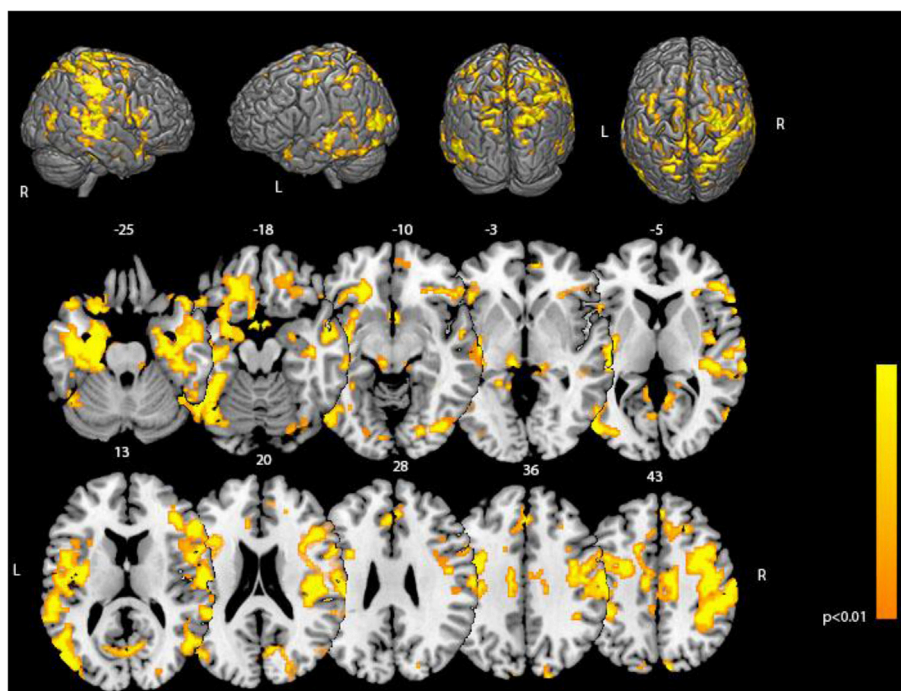


Fig. 3. Group-level significant ($p < 0.01$, family-wise-error corrected using TFCE) patterns of increased activation (orange-yellow) are shown overlaid on a template brain available in MRICroGL. The group-level patterns were obtained from the main effects of microsleeps (combined across rested and sleep-restricted sessions). The slices are labelled with MNI coordinates.

Table 1

Anatomical locations, MNI coordinates (mm), and t -values corresponding to peak values of increased BOLD activity ($p < 0.01$, TFCE corrected) during microsleeps.

Brain Region	Size (Voxels)	t -value	x	y	z
L. Precentral Gyrus	2568	7.17	-10	-24	72
R. Lateral Occipital Cortex	1734	6.1	30	-66	56
L. Hippocampus	1725	7.65	-34	-20	-20
L. Superior Frontal Gyrus	1334	5.95	-20	6	58
L. Lateral Occipital Cortex (Inferior)	566	6.32	-52	-64	6
R. Inferior Temporal Gyrus	281	5.44	52	-6	-42
L. Lateral Occipital Cortex (Superior)	257	5.62	-22	-68	62
R. Superior Frontal Gyrus	145	4.42	16	20	56
R. Occipital Fusiform Gyrus	117	5.82	34	-78	-12
R. Parietal Operculum Cortex	80	4.26	48	-24	22
R. Superior Parietal Cortex	76	3.88	36	-42	42
L. Superior Parietal Cortex	69	3.4	-40	-36	42
R. Planum Temporale	66	3.63	42	-30	6
L. Subcallosal Cortex	38	4.39	-4	28	-22
L. Temporal Pole	34	4.02	-44	10	-36
R. Lateral Occipital Cortex (Superior)	29	3.48	52	-72	18
L. Cingulate Gyrus	23	3.48	-10	-16	42
L. Lingual Gyrus	19	4.21	-8	-52	2
L. Precentral Gyrus	17	3.87	-52	2	32
L. Inferior Frontal Gyrus	15	3.28	-50	18	12
R. Superior Frontal Gyrus	11	3.23	18	26	42

Temporal evolution of inter-network connectivity

In the individuals with microsleeps, dynamic changes in inter-network anti-correlation between the DMN and rFPN networks was associated with temporal fluctuations in tracking error (Fig. 6). The moderate DMN-rFPN anti-correlation observed during the periods of good tracking was reduced with the intrusions of microsleeps increasing tracking errors. However, the correlation between number of microsleeps and degree of changes in DMN-rFPN connectivity and tracking error was

not significant (Spearman's $r = 0.39$, $p = 0.13$).

Temporal evolution of intra-network connectivity

Within the DMN (Fig. 7), temporal changes in intra-network connectivity between the medial-frontal cortex (MFC) and the posterior-cingulate cortex (PCC) were negatively correlated with temporal changes in tracking error across subjects (t -test of r -values, $t = -2.75$, $p = 0.01$). There was no association between changes in connectivity within the rFPN and tracking error.

Discussion

This study investigated changes in neural activity and connectivity during microsleeps in healthy subjects exposed to overnight sleep restriction. By continuously sampling behavioural responsiveness (visuo-motor tracking) and eye-video recording during fMRI scanning, we were able to identify microsleeps and measure corresponding changes in brain activity. We studied performance changes immediately following microsleeps and identified intrinsic functional networks critical for recovery of responsiveness. Furthermore, we were able to map the temporal evolution of inter-network and intra-network connectivity in these functional networks on tonic changes in alertness following sleep restriction. Our observations provide new insight into (i) dynamic shifts in brain activity which occur during the transition from wakefulness to spontaneous microsleeps, (ii) dynamic shifts in brain activity during return to wakefulness/responsiveness following microsleeps, and (iii) how such dynamics are tentatively altered by sleep-restriction.

Consistent with the wake-state instability hypothesis (Doran et al., 2001), we observed that tracking performance (measured using tracking error) following sleep loss was accompanied by mixed periods of drowsy performance, good performance, and intrusion of microsleeps. Performance variability following sleep restriction was greater than performance variability when fully rested, both before and after removing the effects of microsleeps, suggesting that microsleeps are not the only source of variability in performance following sleep loss. There was a large

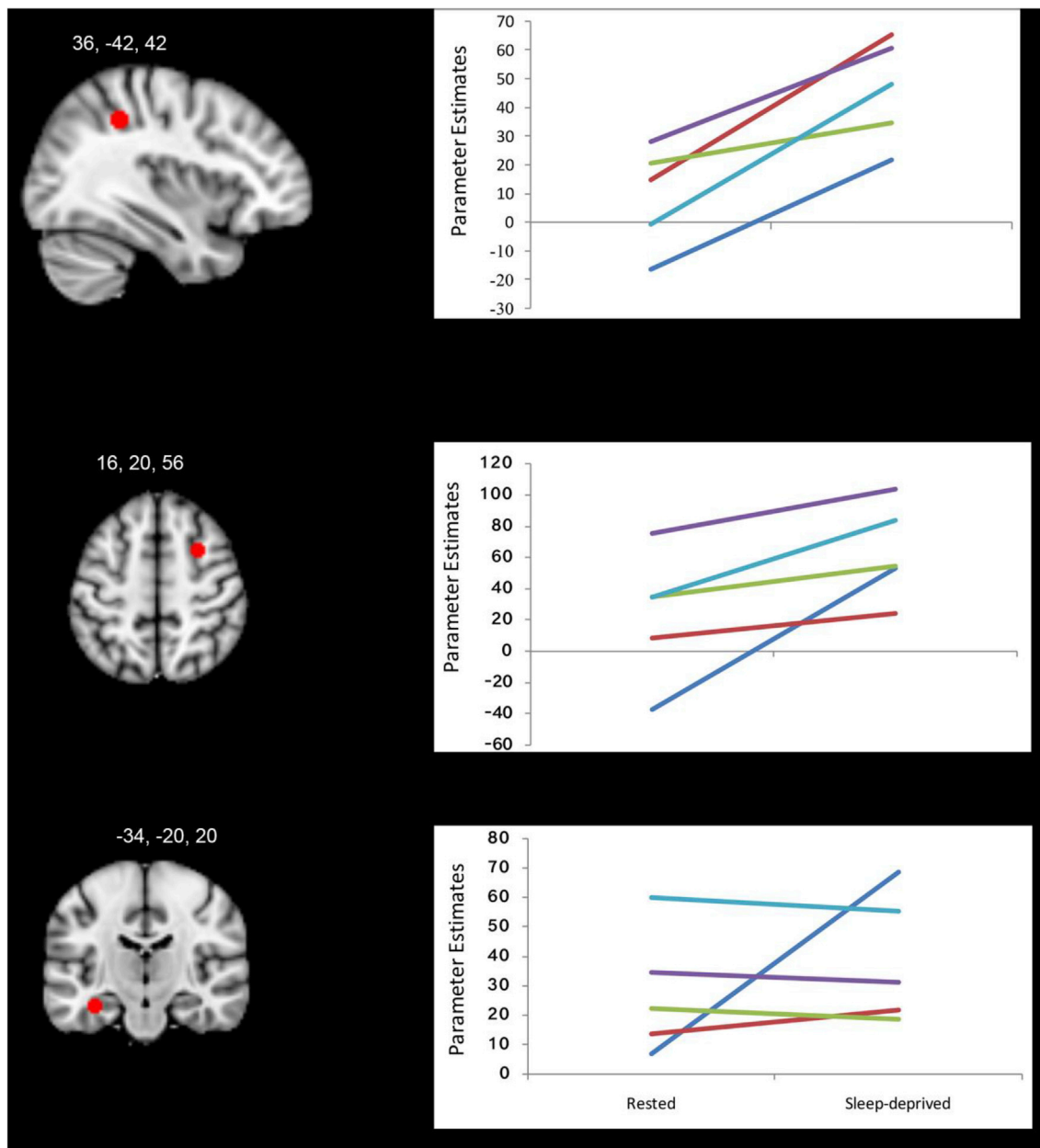


Fig. 4. Microsleep-related fMRI activity (parameter estimates from first-level model) in the right superior-parietal, superior-frontal cortices, and left hippocampus during rested and sleep-deprived sessions in the 5 subjects who had >5 microsleeps in both sessions. The red spheres on the MRI slices represent ROI locations. The fMRI data points from each individual are plotted as separate lines (with different colours).

inter-individual variability in the frequency of microsleeps and in the variability in performance. All of these behavioural changes are consistent with previous studies on sustained attention performance after sleep deprivation (Chee and Tan, 2010; Doran et al., 2001; Drummond et al., 2005; Goel et al., 2009; Innes et al., 2013; Toppi et al., 2016). However, an important distinction of our study was our ability to track behavioural performance at a sub-second level using a specially-designed 2-D continuous tracking task (Poudel et al., 2010, 2014). Two-D tasks not only allows accurate temporal localization of the start and end of transient lapses of responsiveness but also help uncover second-to-second tonic neurobehavioural variability induced by fluctuations in drowsiness (Huang et al., 2005; Peiris et al., 2006).

When the subjects were sleep-restricted, the tracking error immediately following their microsleeps was better than that immediately before those microsleeps. Furthermore, a positive association was observed between the duration of microsleeps and post-microsleep response speed.

This suggests that longer microsleeps provide better responsiveness, at least transiently, following recovery from microsleeps. This, in turn, suggests that microsleeps have intrinsic benefit in terms of temporary dissipation of sleep drive. Dissipation of homeostatic sleep drive following extended wakefulness is driven by the appearance of slow-wave activity (SWA) during sleep (Tononi and Cirelli, 2006). Importantly, other studies suggest that this SWA can occur locally in the brain even when one is awake (Hung et al., 2013; Vyazovskiy et al., 2011). SWA when awake appears due to small groups of fatigued cortical neurons going briefly offline without causing behavioural manifestations of sleep (Vyazovskiy et al., 2011). In contrast, microsleeps cause global slowing of EEG and clear behavioural manifestation of sleep in the eyes and responsiveness (Poudel et al., 2014; Toppi et al., 2016). There is also evidence that at least some microsleeps involve transitory intrusions into Stage-2 sleep (Jonmohamadi et al., 2016). We suggest that microsleeps can provide small and transitory relief from sleep pressure by way of the

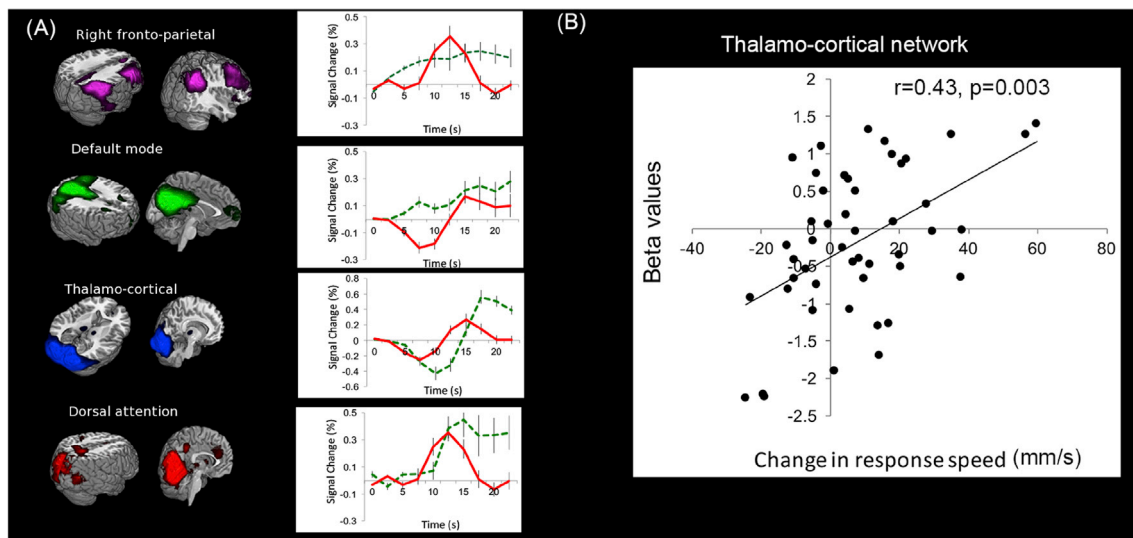


Fig. 5. Transient responses in intrinsic functional networks of interest during microsleeps. (A) Time-courses of transient changes in microsleep-related activity in the right fronto-parietal, default-mode, thalamo-cortical, and dorsal-attention networks when rested (green-dashed line) and sleep-restricted (red line). (B) Correlation between beta values from the thalamo-cortical network (for microsleeps >5 s duration) and change in response speed (mm/s) from the microsleep state to post-microsleep (i.e., post microsleep response speed (averaged for 1 s) minus during microsleep response speed).

same homeostatic mechanism as occurs in global sleep and local sleep. Of course, in the case of microsleeps, this relief is at the cost of a brief loss of consciousness during an active task, which, in turn, could well be at the expense of a fatal accident.

Consistent with previous findings, the neural activity during microsleeps increased in the frontal, parietal, occipital, and para-hippocampal cortices. Importantly, the spatial pattern of activity during microsleeps was observed after excluding regions associated with voluntarily eye closure (Poudel et al., 2010). It is important to note that microsleeps are a complex behaviour and the increase in neural activity seen during microsleeps appears driven by multiple distinct neural processes. Transient eye-closures, which are key behavioural manifestations of microsleeps, are associated with increased activity in multisensory cortical and sub-cortical brain areas and, hence, are major confounds. However, in the present study we excluded regions activated during voluntary eye-closures using a spatial mask derived from a previous study (Poudel et al., 2010). Therefore, the brain regions observed to be active in the present study are specific to microsleeps. A recent study also directly compared activity during spontaneous eye-closures following sleep deprivation with voluntary eye-closure-related activity when rested and reported similar differences (Ong et al., 2015). The struggle to stay awake after sleep deprivation requires individuals to cognitively resist sleep drive, which may manifest as transient increases in activity during microsleep intrusions. This interpretation is supported by findings that individuals able to better maintain wakefulness and performance after sleep restriction have increased blood flow in the fronto-parietal cortex (Drummond et al., 2005; Poudel et al., 2012). The transition from wakefulness to sleep also represents periods of hypnagogic mentation, which are associated with increased activity in brain regions involving sensory processing (Bodizs et al., 2008). Furthermore, detection of response errors, a key behavioural component of recovery from microsleeps, is also associated with increased neural activities in prefrontal and anterior cingulate cortices (Debener et al., 2005). Taken together, the findings suggest that one or more of these processes may drive the large-scale activations observed during microsleeps. Importantly, microsleeps while rested and sleep-restricted appear to be similar in their neural correlates, raising a hypothesis that homeostatic sleep drive has limited effect on the neural signatures of microsleeps. Although, this interpretation is tentative, as the lack of robust differences could be explained by small sample size ($N = 5$).

We found that the temporal patterns of transient activity during

microsleeps differ across intrinsic functional brain networks. Although this finding is exploratory in nature, it is consistent with voxel-wise activity observed during microsleeps. Moreover, the data-driven analysis revealed that while the fronto-parietal and dorsal-attention networks exhibited transient activations, the default-mode and thalamo-cortical networks showed transient reductions in activity followed by hyper-activation. Fronto-parietal and dorsal-attention networks have increased activity during optimal responses in sustained-attention tasks (Ballard et al., 2008; Kim et al., 2006), supporting the role of these networks in cognitive drive to return to wakefulness during microsleeps. In contrast, the ventromedial-prefrontal cortex and posterior-cingulate cortex nodes within the default-mode network exhibit stronger metabolic activity at rest than during cognitive tasks (Raichle et al., 2001). Deactivation of the thalamo-cortical network during microsleeps has also been shown in two previous studies (Ong et al., 2015; Poudel et al., 2014). Although, we did not observe significant deactivation in the voxel-wise analysis (possibly due to lack of power), time-course analysis of the thalamo-cortical network showed a temporal pattern similar to that observed in previous studies. Critically, post-microsleep hyper-activation in the thalamo-cortical network was associated with response speed after recovery, suggesting that responsiveness of thalamo-cortical networks may predict behavioural responsiveness following microsleeps.

Temporal dynamics of the functional connectivity between the rFPN and DMN and within the key hubs in the DMN were associated with the temporal evolution of behavioural performance in each subject. The DMN and rFPN are intrinsically linked in the brain in the form of strong anticorrelations in spontaneous low frequency fluctuations within these networks (Fox et al., 2005). The anticorrelation reflects competitive dynamics between these networks in healthy and alert brain states, which can change with transition to different mental states (Fornito et al., 2012). We specifically observed that the anticorrelation between rFPN and DMN actually decreased with increasing tracking error (reflecting increased microsleeps). This is consistent with previous findings showing that connectivity between the DMN and its anticorrelated network decreases at sleep onset (Samann et al., 2011). Furthermore, a recent study reported that the state of reduced arousal, dominated by eye-lid closures, is associated with decreased anticorrelation between rFPN and DMN (Wang et al., 2016). Within the DMN, we observed that the correlation between the ventromedial-prefrontal cortex (vmPFC) and posterior-cingulate cortex (PCC) decreased with increasing tracking error. Previous studies have shown that connectivity within the DMN is

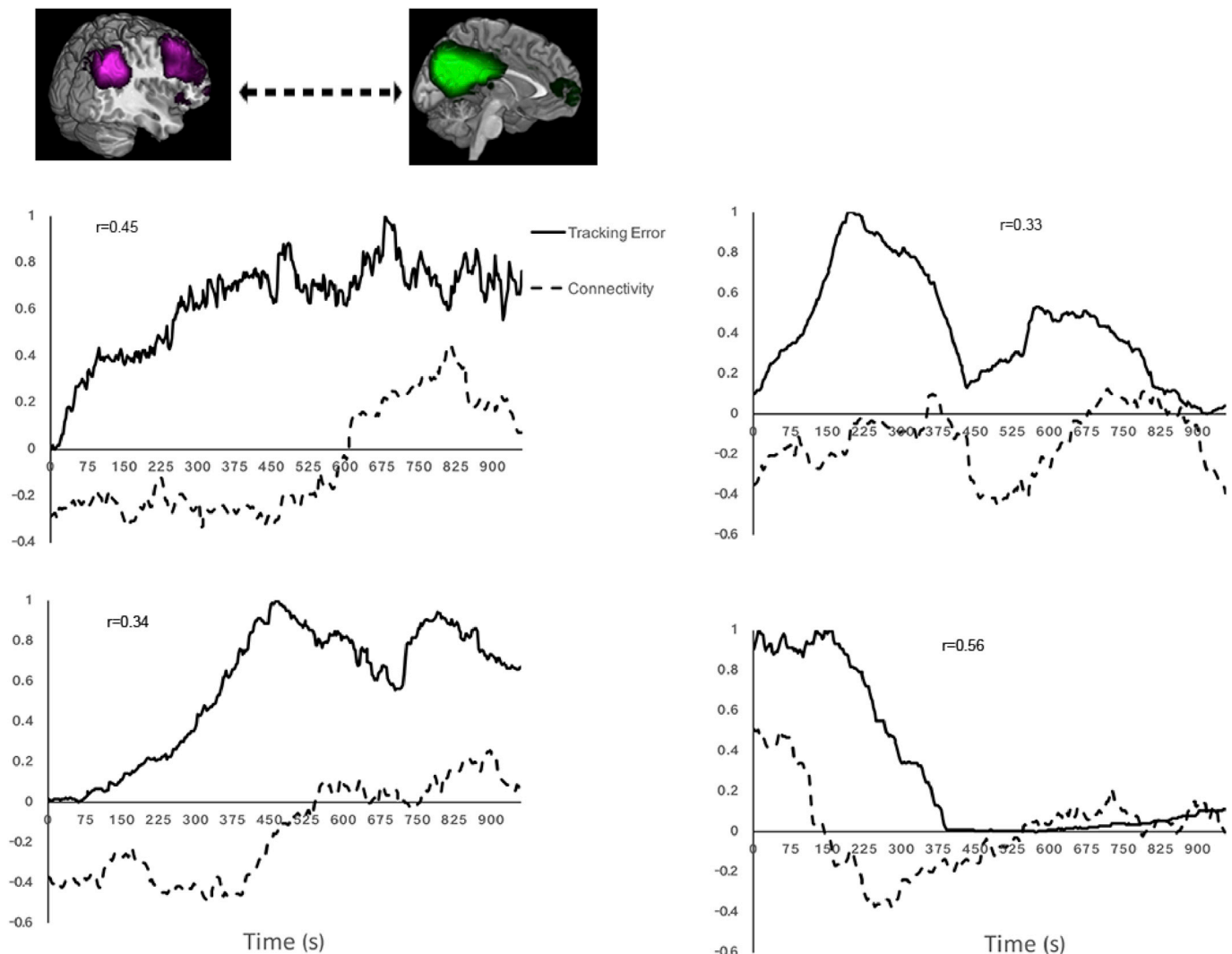


Fig. 6. Relationship between temporal evolution of DMN-rFPN connectivity and tracking error. Example data from 4 representative subjects showing moderate DMN-rFPN anti-correlation during the periods of good tracking performance (reduced tracking error), which lessened with the intrusions of microsleeps (and concomitant increase in tracking errors).

strong in an alert rested state, which remains stable (Horowitz et al., 2008) or may only decrease slightly (Samann et al., 2011) during early sleep stages. Furthermore, consistent with our findings, when hypo-arousal is clearly manifested in eye-lid closures, intra-network connectivity within the DMN decreases (Wang et al., 2016). The current study demonstrates that increased propensity of microsleeps impacts on the stable intra-network dynamics of DMN connectivity (De Havas et al., 2012).

A number of methodological issues in this study need to be addressed. First, the nature of study is such that there is a large inter-individual variability in the number of microsleeps during rested and sleep restricted sessions. Therefore, the reported findings are disproportionately contributed by the individuals who are vulnerable to sleep restriction and have frequent microsleeps. Second, only the limited number of participants ($N = 5$) had microsleeps in both rested and sleep-restricted sessions. Hence, the differences between rested and sleep-restricted conditions should be interpreted with caution. Third, the dynamic functional connectivity analysis performed in the study used a sliding-window approach, with a window size of 4 min. This length was chosen to ensure that functional connectivity changes were not driven by spurious transient events or residual activity from microsleeps. The downside of this is a reduced temporal precision of dynamic functional connectivity, hence diminishing the ability to detect faster temporal

connectivity changes. Fourth, the study relied on the behavioural manifestations to identify the start and end of microsleeps. The behaviourally-defined microsleeps may-not necessarily overlap with the neurophysiological (i.e., 4–7 Hz theta activity) definition of microsleeps. Hence, future studies should co-register EEG with behaviour to identify and separate the microsleeps with clear EEG manifestations. Fifth, due to the limited number of long microsleeps (>5 s) available, we didn't model the onset and end of microsleeps separately. Hence, the pattern of activity observed during microsleeps may include activity at both the onset and end of microsleeps. Finally, it is important to note that the eye-closure maps used in the present study were derived from a separate study published previously (Poudel et al., 2010). Given the inter-individual variability in fMRI spatial maps, this may have led to minor spatial inaccuracies while excluding the eye-closure related activities from microsleep-related activities. Future studies will need to include a separate voluntary eye-closure paradigm within the same group of participants.

In summary, we used fMRI, continuous visuomotor response sampling, and ocular behaviour during fMRI scanning to map neural activity and spontaneous functional connectivity in the brain during transition to microsleeps, both when rested and when sleep-restricted. Our results indicate a distinct pattern of engagement and disengagement of large-scale networks during transition to microsleeps, which also map onto

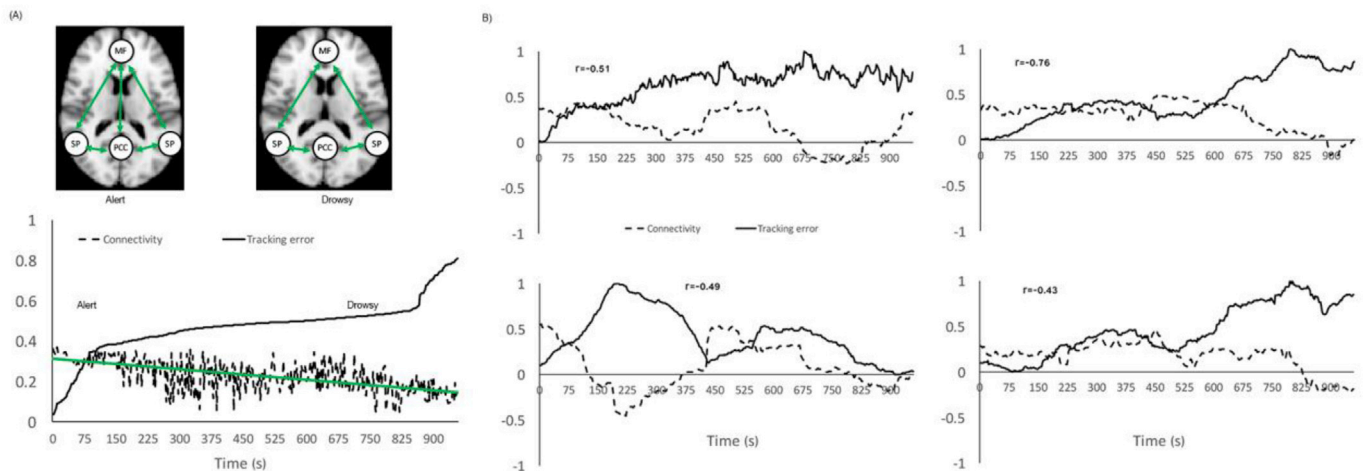


Fig. 7. Temporal evolution of connectivity within the default-mode network. (A) Top panel shows the four nodes, medial-frontal cortex (MFC), posterior-cingulate cortex (PCC), and bilateral superior-parietal (SP) cortex within the default mode network. During alert performance (i.e., low tracking error), the medial-frontal cortex (MFC), posterior-cingulate cortex (PCC), and superior-parietal (SP) nodes within the default mode network were positively correlated. However, with an increased number of microsleeps (i.e., drowsy), the PCC-MFC connection was partially decoupled. The bottom panel shows a plot of sorted average tracking error and corresponding average change in PCC-MFC connectivity (dotted line) within the default-mode network. To generate this figure, changes in tracking error (for every 2.5s) were averaged across participants, scaled (0–1), and sorted. The average change in connectivity (moving window of 4-min and a step of 2.5s) was estimated and sorted.

changes in visuomotor responsiveness. These findings have important implications for our understanding of microsleeps and the development of techniques for EEG-based detection of microsleeps (Ayyagari et al., 2015; Davidson et al., 2007; Peiris et al., 2011) and even prediction of microsleeps (Baseer et al., 2017; Shoorangiz et al., 2016, 2017). Taken together, our findings also raise a compelling possibility that intrusion of microsleeps may provide momentary relief from homeostatic drive to sleep.

Acknowledgements

Funding: This work was supported by the Royal Society of New Zealand Marsden Fund (VDV0801), Canterbury Medical Research Foundation, Lottery Health Research (251144), and Accident Compensation Corporation (09/088), New Zealand.

Appendix A. Supplementary data

Supplementary data related to this article can be found at <https://doi.org/10.1016/j.neuroimage.2018.03.031>.

References

- Akerstedt, T., Gillberg, M., 1990. Subjective and objective sleepiness in the active individual. *Int. J. Neurosci.* 52, 29–37.
- Ayyagari, S., Jones, R., Weddell, S., 2015. Optimized echo state networks with leaky integrator neurons for EEG-based microslepp detection. In: *Proceedings of Annual International Conference of IEEE Engineering in Medicine and Biology Society*, vol. 37, pp. 3775–3778.
- Ballard, J.C., Marker, R.J., Pilato, M.S., Kang, P., Robinson, K.H., Findlay-Lester, R.M., 2008. Time-related fMRI-BOLD signal changes during sustained attention tasks. *Clin. Neurophysiol.* 22, 741.
- Baseer, A., Weddell, S., Jones, R., 2017. Prediction of microsleeps using pairwise joint entropy and mutual information between EEG channels. In: *Proceedings of Annual International Conference of IEEE Engineering in Medicine and Biology Society*, vol. 39, pp. 4495–4498.
- Beckmann, C.F., Smith, S.A., 2004. Probabilistic independent component analysis for functional magnetic resonance imaging. *Ieee Trans. Med. Imaging* 23, 137–152.
- Bodizs, R., Sverteczki, M., Meszaros, E., 2008. Wakefulness-sleep transition: emerging electroencephalographic similarities with the rapid eye movement phase. *Brain Res. Bull.* 76, 85–89.
- Boyle, L.N., Tippin, J., Paul, A., Rizzo, M., 2008. Driver performance in the moments surrounding a microslepp. *Transp. Res. Part F-Traffic Psychol. Behav.* 11, 126–136.
- Chee, M., Tan, J., Zheng, H., Parimal, S., Weissman, D., Zagorodnov, V., Dinges, D., 2008. Lapsing during sleep deprivation is associated with distributed changes in brain activation. *J. Neurosci.* 28, 5519–5528.
- Chee, M.W., Tan, J.C., 2010. Lapsing when sleep deprived: neural activation characteristics of resistant and vulnerable individuals. *Neuroimage* 51, 835–843.
- Davidson, P.R., Jones, R.D., Peiris, M.T.R., 2007. EEG-based lapse detection with high temporal resolution. *Ieee Trans. Biomed. Eng.* 54, 832–839.
- De Havas, J.A., Parimal, S., Soon, C.S., Chee, M.W.L., 2012. Sleep deprivation reduces default mode network connectivity and anti-correlation during rest and task performance. *Neuroimage* 59, 1745–1751.
- Debener, S., Ullsperger, M., Siegel, M., Fiehler, K., Cramon, D.Y.v., Engel, A.K., 2005. Trial-by-Trial coupling of concurrent electroencephalogram and functional magnetic resonance imaging identifies the dynamics of performance monitoring. *J. Neurosci.* 25, 11730–11737.
- Doran, S.M., Van Dongen, H.P., Dinges, D.F., 2001. Sustained attention performance during sleep deprivation: evidence of state instability. *Arch. Ital. Biol.* 139, 253–267.
- Drummond, S.P., Bischoff-Grethe, A., Dinges, D.F., Ayalon, L., Mednick, S.C., Meloy, M.J., 2005. The neural basis of the psychomotor vigilance task. *Sleep* 28, 1059–1068.
- Drummond, S.P.A., Gillin, J.C., Brown, G.G., 2001. Increased cerebral response during a divided attention task following sleep deprivation. *J. Sleep Res.* 10, 85–92.
- Fornito, A., Harrison, B.J., Zalesky, A., Simons, J.S., 2012. Competitive and cooperative dynamics of large-scale brain functional networks supporting recollection. In: *Proceedings of the National Academy of Sciences of the United States of America*, vol. 109, pp. 12788–12793.
- Fox, M.D., Snyder, A.Z., Vincent, J.L., Corbetta, M., Van Essen, D.C., Raichle, M.E., 2005. The human brain is intrinsically organized into dynamic, anticorrelated functional networks. In: *Proceedings of the National Academy of Sciences of the United States of America*, vol. 102, pp. 9673–9678.
- Goel, N., Rao, H., Durmer, J.S., Dinges, D.F., 2009. Neurocognitive consequences of sleep deprivation. *Semin. Neurol.* 29, 320–339.
- Hoddes, E., Dement, W., Zarcone, V., 1972. The development and use of the Stanford sleepiness scale. *Psychophysiology* 9, 150.
- Horowitz, S.G., Fukunaga, M., de Zwart, J.A., van Gelderen, P., Fulton, S.C., Balkin, T.J., Duyn, J.H., 2008. Low frequency BOLD fluctuations during resting wakefulness and light sleep: a simultaneous EEG-fMRI study. *Hum. Brain Mapp.* 29, 671–682.
- Huang, R.S., Jung, T.P., Makeig, S., 2005. Analyzing Event-related Brain Dynamics in Continuous Compensatory Tracking Tasks. 27th Annual International Conference of the IEEE-engineering-in-medicine-and-biology-society. *Ieee*, Shanghai, PEOPLES R CHINA, pp. 5750–5753.
- Hung, C.S., Sarasso, S., Ferrarelli, F., Riedner, B., Ghilardi, M.F., Cirelli, C., Tononi, G., 2013. Local experience-dependent changes in the wake EEG after prolonged wakefulness. *Sleep* 36, 59–72.
- Innes, C.R., Poudel, G.R., Jones, R.D., 2013. Efficient and regular patterns of nighttime sleep are related to increased vulnerability to microsleeps following a single night of sleep restriction. *Chronobiol. Int.* 30, 1187–1196.
- Jenkinson, M., 2003. A fast, automated, n-dimensional phase unwrapping algorithm. *Magn. Reson. Med.* 49, 193–197.
- Jenkinson, M., Bannister, P., Brady, M., Smith, S., 2002. Improved optimization for the robust and accurate linear registration and motion correction of brain images. *NeuroImage* 17, 825–841.
- Johns, M.W., 1991. A new method for measuring daytime sleepiness: the Epworth sleepiness scale. *Sleep* 14, 540–545.
- Jonmohamadi, Y., Poudel, G.R., Innes, C., Jones, R.D., 2016. Microsleeps are associated with Stage-2 sleep spindles from hippocampal-temporal network. *Int. J. Neural Syst.* 26.

- Kim, J., Whyte, J., Wang, J.J., Rao, H.Y., Tang, K.Z., Detre, J.A., 2006. Continuous ASL perfusion fMRI investigation of higher cognition: quantification of tonic CBF changes during sustained attention and working memory tasks. *Neuroimage* 31, 376–385.
- Ong, J.L., Kong, D., Chia, T.T., Tandi, J., Thomas Yeo, B.T., Chee, M.W., 2015. Co-activated yet disconnected-Neural correlates of eye closures when trying to stay awake. *Neuroimage* 118, 553–562.
- Peiris, M.T.R., Davidson, P.R., Bones, P.J., Jones, R.D., 2011. Detection of lapses in responsiveness from the EEG. *J. Neural Eng.* 8.
- Peiris, M.T.R., Jones, R.D., Davidson, P.R., Carroll, G.J., Bones, P.J., 2006. Frequent lapses of responsiveness during an extended visuomotor tracking task in non-sleep-deprived subjects. *J. Sleep Res.* 15, 291–300.
- Poudel, G.R., Innes, C.R., Bones, P.J., Watts, R., Jones, R.D., 2014. Losing the struggle to stay awake: divergent thalamic and cortical activity during microsleeps. *Hum. Brain Mapp.* 35, 257–269.
- Poudel, G.R., Innes, C.R.H., Jones, R.D., 2012. Cerebral perfusion differences between drowsy and nondrowsy individuals after acute sleep restriction. *Sleep* 35, 1085–1096.
- Poudel, G.R., Jones, R.D., Innes, C.R., Watts, R., Davidson, P.R., Bones, P.J., 2010. Measurement of BOLD changes due to cued eye-closure and stopping during a continuous visuomotor task via model-based and model-free approaches. *IEEE Trans. Neural Syst. Rehabil. Eng.* 18, 479–488.
- Raichle, M.E., MacLeod, A.M., Snyder, A.Z., Powers, W.J., Gusnard, D.A., Shulman, G.L., 2001. A default mode of brain function. *Proc. Natl. Acad. Sci. U. S. A.* 98, 676–682.
- Samann, P.G., Wehrle, R., Hoehn, D., Spoormaker, V.I., Peters, H., Tully, C., Holsboer, F., Czisch, M., 2011. Development of the Brain's default mode network from wakefulness to slow wave sleep. *Cereb. Cortex* 21, 2082–2093.
- Shoorangiz, R., Weddell, S., Jones, R., 2017. Bayesian multi-subject factor analysis to predict microsleeps from EEG power spectral features. In: *Proceedings of Annual International Conference of IEEE Engineering in Medicine and Biology Society*, vol. 39.
- Shoorangiz, R., Weddell, S.J., Jones, R.D., 2016. Prediction of microsleeps from EEG: preliminary results. In: *38th Annual International Conference of the IEEE-engineering-in-medicine-and-biology-society (EMBC)*, Orlando, FL, pp. 4650–4653.
- Smith, S.M., Fox, P.T., Miller, K.L., Glahn, D.C., Fox, P.M., Mackay, C.E., Filippini, N., Watkins, K.E., Toro, R., Laird, A.R., Beckmann, C.F., 2009. Correspondence of the brain's functional architecture during activation and rest. *Proc. Natl. Acad. Sci. U. S. A.* 106, 13040–13045.
- Smith, S.M., Nichols, T.E., 2009. Threshold-free cluster enhancement: addressing problems of smoothing, threshold dependence and localisation in cluster inference. *Neuroimage* 44, 83–98.
- Tomasi, D., Wang, R.L., Telang, F., Boronikolas, V., Jayne, M.C., Wang, G.-J., Fowler, J.S., Volkow, N.D., 2008. Impairment of attentional networks after 1 night of sleep deprivation. *Cereb. Cortex* 19, 223–240.
- Tononi, G., Cirelli, C., 2006. Steep function and synaptic homeostasis. *Sleep. Med. Rev.* 10, 49–62.
- Toppi, J., Astolfi, L., Poudel, G.R., Innes, C.R.H., Babiloni, F., Jones, R.D., 2016. Time-varying effective connectivity of the cortical neuroelectric activity associated with behavioural microsleeps. *Neuroimage* 124, 421–432.
- Vyazovskiy, V.V., Olcese, U., Hanlon, E.C., Nir, Y., Cirelli, C., Tononi, G., 2011. Local sleep in awake rats. *Nature* 472, 443–447.
- Wang, C., Ong, J.L., Patanaik, A., Zhou, J., Chee, M.W., 2016. Spontaneous eyelid closures link vigilance fluctuation with fMRI dynamic connectivity states. *Proc. Natl. Acad. Sci. U. S. A.* 113, 9653–9658.